HHS Public Access

Author manuscript

J Immunol. Author manuscript; available in PMC 2024 June 01.

Published in final edited form as:

J Immunol. 2023 June 01; 210(11): 1752–1760. doi:10.4049/jimmunol.2200927.

The chromatin regulator Mll1 supports T follicular helper cell differentiation by controlling expression of Bcl6, LEF-1, and TCF-1

Simon Bélanger[*,#], **Sonya Haupt**[*,†], **Caterina E. Faliti**[*], **Adam Getzler**[‡], **Jinyong Choi**[*,§], **Huitian Diao**[‡], **Pabalu P. Karunadharma**[¶], **Nicholas A. Bild**[¶], **Matthew E. Pipkin**[‡], **Shane Crotty**[*,||]

[*]Center for Infectious Disease and Vaccine Research, La Jolla Institute for Immunology (LJI), La Jolla, CA, USA

[†]Biomedical Sciences (BMS) Graduate Program. School of Medicine, University of California, San Diego (UCSD), La Jolla, CA, 92037, USA

[‡]Department of Immunology and Microbiology, The Scripps Research Institute, Jupiter, FL, 33458, USA

[§]Department of Microbiology, Department of Biomedicine & Health Sciences, College of Medicine, The Catholic University of Korea, Seoul, 03083, Republic of Korea

[¶]Genomics Core, The Scripps Research Institute, Jupiter, FL, 33458, USA

[||]Department of Medicine, Division of Infectious Diseases and Global Public Health, University of California, San Diego (UCSD), La Jolla, CA, 9203,7USA

Abstract

T follicular helper (T_{FH}) cells are essential for developing protective antibody responses following vaccination. Greater understanding of the genetic program leading to T_{FH} differentiation is needed. Chromatin modifications are central in the control of gene expression. However, detailed knowledge of how chromatin regulators (CRs) regulate differentiation of T_{FH} cells is limited. We screened a large shRNA library targeting all known CRs in mouse and identified the histone methyltransferase Mll1 as a positive regulator of T_{FH} differentiation. Loss of Mll1 expression reduced formation of T_{FH} cells following acute viral infection or protein immunization. In addition, expression of the T_{FH} lineage-defining transcription factor Bcl6 was reduced in the absence of Mll1. Transcriptomics analysis identified *Lef1* and *Tcf7* as genes dependent on Mll1

Correspondence to: Shane Crotty, PhD, La Jolla Institute for Immunology, 9420 Athena Circle, La Jolla, CA 92037, shane@lji.org, (858) 752-6816, (858) 752-6993 (fax).

[#]Current address: VIR Biotechnology, San Francisco, CA, 94158, USA

COMPETING INTERESTS

S.B. is a current employee of VIR Biotechnology and may possess shares of VIR Biotechnology.

S.B. designed and performed the experiments, analyzed data and wrote the manuscript; S.H. performed the experiments and analyzed data; C.E.F. and J.C. generated reagents; A.G., H.D., P.P.K. and N.A.B. performed and analyzed the next generation sequencing of the shRNA screen; M.E.P. supervised sequencing analysis; S.C. designed the study, supervised the work and wrote the manuscript.

RNA-seq data are deposited to the Gene Expression Omnibus (GEO) under the GSE226341 accession number (https://www.ncbi.nlm.nih.gov/geo/query/acc.cgi?acc=GSE226341)

for their expression, which provides one mechanism for the regulation of T_{FH} differentiation by Mll1. Taken together, CRs such as Mll1 substantially influence T_{FH} differentiation.

INTRODUCTION

High-affinity antibodies are central to immune protection elicited following vaccination. Germinal center (GCs) are essential for the production of such antibodies (1). T follicular helper CD4 T cells (T_{FH}) cells provide essential help signals to antigen-specific B cells for the formation of germinal center B cells (B_{GC}) that culminate in the formation of long-lived antibody-secreting plasma cells and memory B cells (1). Differentiation of CD4 T cells into T_{FH} cells is initiated upon interaction of activated CD4 T cell with antigen-presenting dendritic cells (1). Expression of the transcriptional repressor Bcl6 in CD4 T cells induces the T_{FH} transcriptional program. Bcl6 directs T_{FH} differentiation by suppressing alternative T helper cell fates and by promoting expression of gene products associated with T_{FH} cells and function (1–5). Other transcription factors such as LEF-1/TCF-1 (*Lef1*/*Tcf7*) (6–8), Batf (9, 10), Maf (11, 12) or E proteins (13, 14) play critical roles in supporting T_{FH} differentiation. These transcription factors are balanced by inhibitors of T_{FH} differentiation such as Blimp-1 (5) and Klf2 (2, 15).

Differentiation of CD4 T cells into a wide variety of helper subsets is tightly controlled by chromatin modifications (16). Transcription factors driving T_{FH} differentiation have been thoroughly characterized, but the role of epigenetics in controlling this process remains mostly unexplored. T_{FH} cells possess cell type-specific enhancers identified by monomethylation of histone 3 lysine 4 (H3K4Me) and acetylation at lysine 27 of histone 3 (H3K27Ac) (17, 18). Additionally, T_{FH} cells possess unique patterns of chromatin accessibility (2, 17). All of the above suggest an epigenetic program specific for T_{FH}.

Bcl6 plays a central role in establishing the T_{FH}-specific epigenetic program. The middle domain of Bcl6, which recruits the corepressor MTA3, is necessary for full activity of Bcl6 and proper formation of T_{FH} cells (19). Additionally, depletion of the corepressor NCoR1, or deletion of BCoR, impairs T_{FH} formation (2, 20). TCF-1 recruits the histone methyltransferase EZH2 to activate *Bcl6* expression (21), and absence of EZH2 abrogates T_{FH} differentiation (21, 22). The histone methyltransferase Nsd2 influences T_{FH} differentiation by promoting expression of *Bcl6* in the early stages of CD4 T cell activation (23). Bcl6, of course, is not the only T_{FH}-associated target of CRs. The histone demethylase UTX impacts T_{FH} differentiation by regulating *Il6ra* expression (24). We sought to identify novel CRs essential for T_{FH} formation. To this end, we adapted our *in vivo* shRNA-based screening approach (25) to survey a library of shRNAmir targeting all known CRs in mouse. We identified Mll1 (Mixed Lineage Leukemia 1) as a positive regulator of T_{FH} differentiation and function.

MATERIALS AND METHOD

Mice, LCMV infection and protein immunization.

SMARTA mice (transgenic expression of an I-A^b-restricted TCR specific for LCMV glycoprotein amino acids 66–77) (26) and CD45.1^+ mice were on a full C57BL/6 background and bred in-house. C57BL/6 and $Cas9^{Tg}$ mice (JAX stock #028555) were purchased from the Jackson laboratory. Both male and female mice were used throughout the study, with sex and age matched T cell donors and recipients. All mice were maintained in specific-pathogen-free facilities and used according to protocols approved by the animal care and use committees of LJI. Mice were infected via the intraperitoneal route with 2×10^5, 4×10^5 or 5×10^5 plaque-forming units of LCMV-Armstrong for days 6, 4 or 3 analysis, respectively. 10 μg of KLH conjugated to $gp_{66–77}$ peptide of LCMV mixed with 2.5 μg of SMNP (27) in 100 μL PBS was injected at the base of tail. 1 mg BrdU in PBS was injected via intraperitoneal route 16 hours before analysis.

In vivo shRNA screen.

We included a set of 42 control shRNAmir-RV (Supplemental Table 1). 322 CRs genes expressed in mouse are targeted by 3 or 4 shRNAmir each for a total of 1230 shRNAmir-RV in the library (Supplemental Table 1). The initial screen was performed twice as previously described (25). Subsequent screens were modified as follows. Equal amounts of every shRNAmir were pooled to create 22 tubes. PLAT-E cells were transfected with 2 μg of pooled shRNAmir (1 pool/well) and 1 μg pCL-Eco plasmids. Anti-CD3/CD28 activated SMARTA CD4 T cells were transduced once with RV supernatant. 5×10^5 sorted cells were transferred into 20 recipient mice by intravenous injection. An aliquot of $1.1–1.5\times10^6$ sorted cells was saved for RNA isolation (Input). Mice were infected with 2×10^6 PFU LCMV-Armstrong 4 days after transfer.

3 days after infection, spleens were isolated and pooled. CD45.1^+ SMARTA cells were pre-enriched and sorted into CXCR5^+SLAM^{lo} T_{FH} and CXCR5^-SLAM$^+$ T_H1 SMARTA cells. 1.7×10^5 T_{FH} and 1.6×10^6 T_H1 cells were sorted for the first screen. 7.2×10^5 T_{FH} and 3.2×10^6 T_H1 cells were sorted for the second screen. Total RNA was isolated using mirVana miRNA Isolation Kit (Invitrogen). RNA was quantified with High Sensitivity RNA ScreenTape kit and TapeStation (Agilent). 70 ng of RNA was used to synthesize cDNA using random oligonucleotides in triplicate reactions that were subsequently pooled.

Sequencing the shRNAmir library.

The amount of shRNAmir-derived cDNA template in each sample preparation was quantified using qPCR and a standard curve prepared from known molar amounts of gel-purified shRNAmir amplicons. To build shRNAmir amplicon libraries capturing passenger strand sequences, an amount of cDNA template in each sample resulting in equivalent amplification to previously analyzed libraries amplified from 100 ng of total genomic DNA template from transduced T cells was amplified using primers including Illumina P5 adapter (5’-AATGATACGGCGACCACCGAGATCTACACTCTTTCCCTACACGACGCTCTTCCGATCTCTCGAGAAGGTATATTGCT-3’) and P7 (5’-

CAAGCAGAAGACGGCATACGAGATNNNNNNGTGACTGGAGTTCAGACGTGTGCT CTTCGATCTACATCTGTGGCTTCACTA-3') adapter sequences. The miR30 (P5) and shRNAmir-loop (P7) annealing sequences are underlined and the custom barcode is indicated (Ns). Sequencing libraries were amplified in triplicate reactions using Phusion High-Fidelity DNA polymerase in 1X HF buffer for 24 PCR cycles. Replicate reactions were pooled, purified with 1.6X AMPure XP beads (Beckman Coulter), and quantified with Qubit DNA assay and Agilent 2100 Bioanalyzer (Agilent Technologies, Inc.). The individually barcoded libraries were pooled in equimolar ratios, mixed with separate base-balanced libraries to increase diversity and sequenced on the NextSeq 500 at 1.8 pM concentration with paired-end 75bp reads.

A FASTA formatted reference database comprising 97mer sequences of all analyzed shRNAmirs in the library was built. Raw sequencing reads were merged using FLASH and the merged reads were compared to the reference database using nucleotide BLAST. Only the top alignment for each read was retained and the number of times each reference sequence was aligned in each sample library was counted and reported. Normalized reads for all shRNAmir targeting the same gene were averaged to create a single gene read number and gene log2 T_{FH}/T_H1 ratios were calculated.

Retroviral vectors, transductions and cell transfers.

pMIG, *Lef1*, *Tcf7*-p45 and *Bcl6* pMIG were described previously (6, 7, 19). Guide RNAs were selected by CHOP-CHOP (https://chopchop.cbu.uib.no) and cloned into the BbsI site of a modified LMPd-Ametrine vector. Transduction and transfer of CD4 T cells were performed as previously detailed (25). Transferred cells were allowed to rest in host mice for 3–4 days before infection or immunization. 2×10^4, 5×10^4 or 4×10^5 transduced $CD4^+$ T cells were transferred for day 6, 4 or 3 analysis, respectively. For protein immunization, 2×10^5 transduced cells were transferred. For T_H1 cultures, cells were cultured in the presence of 10 ng/mL IL-12 (Peprotech) and 10 μg/mL anti-IL-4 (R&D Systems).

Flow cytometry and antibodies.

Single-cell suspensions of spleen or draining inguinal lymph nodes were prepared by standard gentle mechanical disruption. Surface staining for flow cytometry was done with monoclonal antibodies against CD4 (RM4–5, 1:400), CD8 (53–6.7, 1:400), CD45.1 (A20, 1:400), B220 (RA3–6B2, 1:400) (eBiosciences); PSGL-1 (2PH1, 1:400), (from BD Biosciences); SLAM (TC15–12F12.2, 1:400), CD25 (PC61, 1:400), CD44 (IM7, 1:400) (BioLegend). CXCR5 staining was done using biotinylated anti-CXCR5 (SPRCL5, eBioscience), followed by PE-Cy7-, BV421- or APC-labeled streptavidin (BioLegend). Intranuclear staining was performed with a monoclonal antibody to Bcl6 (K112–91, BD Biosciences), TCF1 (C63D9), LEF-1 (C12A5, Cell Signaling) or Blimp-1 (5E7, BioLegend), and the Intracellular Fixation & Permeabilization Buffer Set (Invitrogen). For measurement of cytokines, cells from spleen were cultured with 10 μg/ml gp_{66} peptide and Brefeldin A. Intracellular staining for cytokines was performed with monoclonal antibody to IFN-γ (XMG1.2), CD40L (MR1), IL-2 (JES6–5H4, Invitrogen) and recombinant mouse IL-21 receptor Fc (R&D Systems), followed by anti-human IgG (Invitrogen), using the Fixation/Permeabilization buffer kit (BD Biosciences). BrdU staining was performed with

the BrdU Flow Kit (BD Biosciences). Stained cells were analyzed using LSRII or Celesta (BD Biosciences) and FlowJo software (TreeStar). Anti-TBP (ab63766, Abcam) and anti-Mll1 (14689, Cell Signaling Technologies) were used in western blots.

RNA-Seq.

CD45.1$^+$ gRNA$^+$ Cas9^{Tg} SMARTA cells were pre-enriched from spleens pooled from 4 mice per group. 5,000–150,000 CXCR5$^+$SLAM^{lo} T_{FH}, CXCR5$^-$SLAM$^+$ T_H1 SMARTA cells, or naïve SMARTA cells were sorted into Trizol LS (Invitrogen). RNA-Seq was performed as previously described (2). 0.5 ng cDNA was used to prepare a standard Nextera XT sequencing library (Nextera XT DNA library preparation kit and index kit; Illumina). Libraries were sequenced using a HiSeq2500 (Illumina) to generate 50-bp single-end reads, generating median of >17 million mapped reads per sample. Three biological replicates were generated for T_{FH} and T_H1 samples. RNA-Seq was analyzed as previously described (2) except for the following modifications. The reads were aligned with the mm10 reference genome using STAR (v 2.6.1) and the RefSeq gene annotation downloaded from the UCSC Genome Bioinformatics site. Read counts to each genomic feature were obtained with the featureCounts (v 1.6.5) using the default option along with a minimum quality cut off (Phred > 10). We considered genes differentially expressed between two groups of samples when the DESeq2 analysis resulted in an adjusted p-value of <0.05 and the difference in gene expression was 1.4-fold. TPMs were calculated. Gene Set Enrichment Analysis (GSEA) was run on gene lists with GSEA v3.0 (Broad Institute, Inc.). Gene signatures from *in vitro* T_H2, T_{REG}, Bcl6-bound gene list from human tonsil GC-T_{FH} (18), Blimp-1-bound genes from activated CD8 T cells (28), or from *in vitro*-differentiated T_H17 (29) and genes signatures from T_{FH}, T_H1 and *Tcf7*$^{-/-}$*Lef1*$^{-/-}$ GC-T_{FH} isolated after LCMV-Arm infection and from *in vitro*-differentiated *Lef1*$^+$-RV T_H1 (6) were previously published.

Statistical Methods.

Statistical tests were performed using Prism 8.0 (GraphPad). Significance was determined by unpaired Student's *t*-test with a 95% confidence interval, by one-way ANOVA with Tukey's multiple comparisons test or by two-way ANOVA with Sidak's multiple comparisons test. *p<0.05, **p<0.01, ***p<0.001 and ****p<0.0001.

RESULTS

shRNA screen for chromatin regulators of early T_{FH} differentiation

To discover novel CRs regulating T_{FH} differentiation, we generated an shRNAmir retroviral vector (RV) library targeting all known mouse CRs, 322 genes, each targeted by 3–4 shRNAmir for a total of 1230 shRNAmir-RVs. (Fig. 1a). Briefly, LCMV gp66–77-specific TCR transgenic SMARTA CD4 T cells were transduced once with shRNAmir-RV-containing supernatant. shRNAmir-RV$^+$ SMARTA CD4 T cells were sorted based on Ametrine marker expression and adoptively transferred into recipient C57BL/6 mice (Fig. 1b). Total RNA was isolated from an aliquot of CD4 T cells for the Input sample. Recipient mice were infected with LCMV-Arm and, three days after infection, SMARTA CD4 T cells were sorted into CXCR5$^+$SLAM^{lo} T_{FH} and CXCR5$^-$SLAM$^+$ T_H1 populations (Fig. 1c). cDNA sequencing libraries were prepared for the SMARTA Input, T_{FH} and T_H1

samples. Sequenced cDNA was aligned to a list of all shRNAmir sequences in the library to determine read counts for every shRNAmir in the library. The screen was performed twice in independent experiments.

We calculated Z score values of the T_{FH}/T_H1 ratio for every shRNAmir in the library. Direct comparison of Z scores per shRNAmir construct was not informative (Fig. 1d). It is possible that differences in shRNA knockdown efficacy was the source of the variability. We averaged the reads numbers for each shRNA targeting the same gene to create a single Z score for each targeted gene. We hypothesized that calculating a single Z score value for each targeted gene would reduce variability and be more informative. This analysis method showed improved reproducibility between experiments (Fig. 1e, Supplemental Table 1). We assessed the gene Z score distribution of known positive and negative regulators of T_{FH} differentiation. *Bcl6* and *Itch* had negative Z score values in both experiments, indicating their shRNAmir constructs were depleted from the T_{FH} population (Fig. 1e), consistent with their known roles as positive T_{FH} regulators (3–5, 30). Conversely, *Prdm1*, *Tbx21* and *Id2* had positive Z score values, indicative of enrichment in T_{FH} cells (Fig. 1e), consistent with their known roles in directly inhibiting T_{FH} differentiation or promoting T_H1 cells (5, 13, 31). We then filtered the gene Z score data for novel regulators of T_{FH} differentiation by ranking genes depleted from T_{FH} cells. The gene coding for the histone methyltransferase Mll1 was one of the most depleted genes from T_{FH} cells, with Z score values of −1.4 and −4.8, suggesting Mll1 is a positive regulator of T_{FH} differentiation (Fig. 1e). Mll1 methylates lysine 4 of histone 3 (H3K4), a mark associated with active transcription, and assembles with numerous regulatory proteins such as RbBP5, Wdr5, Ash2l, Dpy30 and Menin-1 (32). Mll1 regulates the expression of T_H1 and T_H2 cytokines in CD4 T cells (33, 34) but a role for Mll1 in T_{FH} was unknown. Our shRNA library included shRNA for the Ezh2 and NCoR1, two CR known to regulate Tfh differentiation (2, 23). NCoR1 had Z score values of −0.50 and −2.46 while Ezh2 had Z score values of −1.29 and −0.91 suggesting our screen can detect CRs known to regulate T_{FH} differentiation.

Loss of *Mll1* impairs early T_{FH} differentiation

In published RNA-Seq data (2, 6), we observed that *Mll1* is expressed at similar levels between naive CD4, T_{FH} and T_H1 cells (Supplemental Fig. 1a). Two shRNAmirs that efficiently inhibited Mll1 expression *in vitro* were tested individually for their effect on T_{FH} differentiation *in vivo* (Supplemental Fig. 1b). We transduced SMARTA CD4 T cells with sh*Mll1*-RV or sh*Cd8*-RV, transferred the SMARTA CD4 T cells into C57BL/6 mice, and analyzed T_{FH} differentiation 3 days after infection with LCMV-Arm. sh*Mll1*$^+$ SMARTA CD4 T cells exhibited a significantly smaller early T_{FH} cell population ($CXCR5^+CD25^-$ or $CXCR5^+Bcl6^+$) when compared to sh*Cd8*$^+$ SMARTA cells (Fig. 2a, b, Supplemental Fig. 1c, d). shRNAmirs targeting *Mll1* had a small but significant impact on the accumulation of SMARTA CD4 T cells *in vivo* (Fig. 2c, Supplemental Fig. 1e, f). Importantly, we observed reduced expression of Bcl6 in *Mll1*-deficient $CXCR5^+CD25^-$ early T_{FH} cells (Fig. 2d). These results confirmed the identification of Mll1 as a novel positive regulator of T_{FH} differentiation after LCMV infection.

We next sought to confirm the role of Mll1 using an independent experimental approach. Cas9^{Tg} SMARTA CD4 T cells transduced with a control g*Cd8*-RV or g*Mll1*-RV (Supplemental Fig. 1g) were transferred into C57BL/6 mice and analyzed 3 days after LCMV-Arm infection. g*Mll1*$^{+}$ Cas9^{Tg} SMARTA CD4 T cells had substantially reduced potential to differentiate into CXCR5^{+}CD25^{-} or CXCR5^{+}Bcl6^{+} T_{FH} cells (Fig. 2e, f, Supplemental Fig. 1h, i). Accumulation of g*Mll1*$^{+}$ Cas9^{Tg} SMARTA CD4 T cells was normal after infection (Fig. 2g, Supplemental Fig. 1j). Bcl6 expression was also significantly reduced in g*Mll1*$^{+}$ CXCR5^{+}CD25^{-} cells (Fig. 2h). Thus, disruption of *Mll1* expression by gRNA phenocopied shRNA-mediated knockdown of *Mll1*, establishing Mll1 as a novel positive regulator of T_{FH} differentiation.

Reduced peak T_{FH} differentiation in *Mll1*-deficient CD4 T cells

To assess if Mll1 is dispensable for later stages of T_{FH} differentiation, we analyzed T_{FH} differentiation of *Mll1*-deficient CD4 T cells 6 days after infection. Compared to control sh*Cd8*$^{+}$ cells, sh*Mll1*$^{+}$ SMARTA CD4 T cells showed impaired formation of T_{FH} cells (CXCR5^{+}SLAM^{lo}, Fig. 3a). We next analyzed formation of GC-T_{FH}. The percentages of CXCR5^{+}Bcl6^{+} GC-T_{FH} cells in sh*Mll1*$^{+}$ SMARTA CD4 T cells were comparable to those of control sh*Cd8*$^{+}$ SMARTA (Fig. 3b). Unlike what we observed at 3 days post infection, the reduction in T_{FH} differentiation was coupled to a significant decrease in the accumulation of sh*Mll1*$^{+}$ SMARTA CD4 T cells by day 6 (Fig. 3c, Supplemental Fig. 1k).

gRNA-mediated disruption of Mll1 also significantly reduced CXCR5^{+}SLAM^{lo} T_{FH} differentiation 6 days after LCMV infection (Fig. 3d). g*Mll1*$^{+}$ Cas9^{Tg} SMARTA CXCR5^{+}Bcl6^{+} GC-T_{FH} cells were reduced compared to g*Cd8*$^{+}$ (Fig. 3e). These results suggest that Mll1 mostly regulates T_{FH} differentiation with less impact on GC-T_{FH} differentiation because a reduction in CXCR5^{+}Bcl6^{+} GC-T_{FH} was observed only in g*Mll1*$^{+}$ Cas9^{Tg} SMARTA CD4 T cells but not in sh*Mll1*$^{+}$ SMARTA CD4 T cells. g*Mll1*$^{+}$ Cas9^{Tg} SMARTA CD4 T cells also accumulated significantly less than g*Cd8*$^{+}$ Cas9^{Tg} SMARTA CD4 T cells (Fig. 3f). These results showed that Mll1 is a positive regulator of T_{FH} differentiation after an acute viral infection.

We next tested *Mll1* disruption in the context of protein immunization. C57BL/6 mice that received g*Cd8*$^{+}$ or g*Mll1*$^{+}$ Cas9^{Tg} SMARTA CD4 T cells were immunized subcutaneously with KLH conjugated to $GP_{66–77}$ peptide from LCMV (GP-KLH) mixed with the SMNP adjuvant (saponin monophosphoryl lipid A nanoparticle). Draining lymph nodes were harvested for analysis 8 days later. Differentiation of g*Mll1*$^{+}$ Cas9^{Tg} SMARTA CD4 T cells into CXCR5^{+}PSGL-1^{lo} T_{FH} cell was reduced following immunization (Fig. 3g) while accumulation of *Mll1*-deficient SMARTA CD4 T cells was not compromised (Fig. 3h). These experiments demonstrate a role for Mll1 in T_{FH} cell differentiation in different contexts.

We tested if reduced proliferation of *Mll1*-deficient CD4 T cells was causing their reduced accumulation after LCMV infection. Four days after infection, total sh*Mll1*$^{+}$ SMARTA CD4 T cells showed significantly reduced incorporation of BrdU when compared to sh*Cd8*$^{+}$ SMARTA cells (Fig. 3i). The decrease in BrdU incorporation was observed for both CXCR5^{+}SLAM^{lo} T_{FH} and CXCR5^{-}SLAM^{+} $T_{H}1$ cells (Fig. 3j, k). These results indicate

that Mll1 is required for optimal proliferation of CD4 T cells following infection and suggest that the reduced T_{FH} differentiation of sh*Mll1*$^{+}$ SMARTA CD4 T cells was not caused by a selective proliferation defect of T_{FH} cells. These experiments demonstrated the importance for Mll1 in supporting T_{FH} differentiation.

Mll1 is required for proper IL-21 expression

To test the functionality of *Mll1*-deficient T_{FH} cells, we assessed cytokine production in sh*Cd8*$^{+}$ and sh*Mll1*$^{+}$ SMARTA CD4 T cells 6 days after infection. A substantial fraction of IL-21-producing cells were observed in control sh*Cd8*$^{+}$ SMARTA, but IL-21 expression was greatly reduced in sh*Mll1*$^{+}$ SMARTA (Fig. 4a, Supplemental Fig. 2a). Expression of CD40L or IFN-γ was not affected by loss of Mll1 (Fig. 4b, Supplemental Fig. 2b). Production of IL-2, whose gene is immediately adjacent to *Il21*, was mostly unaffected by *Mll1*-deficiency (Supplemental Fig. 2c). IL-21 expression was similarly disrupted in g*Mll1*$^{+}$ Cas9^{Tg} SMARTA CD4 T cells (Fig. 4c). A small but significant reduction in CD40L was observed while IFN-γ production was not significantly impacted (Fig. 4d, Supplemental Fig. 2d). IFN-γ expression in T_H1 cells in response to LCMV infection was also reduced after gRNA-mediated abrogation of *Mll1* expression (Supplemental Fig. 2e, f) similar to what was observed in *Mll1*$^{+/-}$ CD4 T cells responding to tuberculosis antigens (34).

Notably, we observed reduction of IL-21 production by both T_H1 and T_{FH} cells (Fig. 4e), suggesting that Mll1 regulates IL-21 production independently of T_{FH} differentiation. We next tested if Mll1 is required for IL-21 production in a system independent of T_{FH} differentiation. *In vitro* sh*Mll1*$^{+}$ T_H1 cells and g*Mll1*$^{+}$ Cas9^{Tg} T_H1 cells exhibited impaired IL-21 expression (Fig. 4f, g). Impacts on IFN-γ *in vitro* were variable with sh*Mll1*$^{+}$ T_H1 producing normal levels of IFN-γ while IFN-γ production was reduced in g*Mll1*$^{+}$ T_H1 (Supplemental Fig. 2g, h). Altogether, these results demonstrate that IL-21 production by CD4 T cells depends on Mll1.

Mll1-deficient T_{FH} cells have a dysregulated T_H1 genetic program

To gain further understanding of the function of Mll1, we performed a transcriptomics analysis of *Mll1*-deficient T_{FH} and T_H1 cells (Fig. 5a). *Mll1*-deficient T_{FH} cells had expression changes of a select number of genes in comparison to control T_{FH} cells (89 upregulated and 29 downregulated genes, $|FC| > 1.4$, padj < 0.05, Fig. 5b, c). In T_H1 cells, loss of Mll1 resulted in the downregulation of 91 and the upregulation of 72 genes (Fig. 5b, c). We next asked how different gene expression signatures associated with CD4 T cell subsets were affected by loss of MLL1 expression. We performed gene set enrichment analysis of T_{FH}, T_H1, T_H17, T_H2 and T_{reg} gene signatures against control and *Mll1*-deficient T_H1 and T_{FH} populations. In these analyses, a negative normalized enrichment score (NES) denotes enrichment of the indicated gene signature in the g*Mll1*$^{+}$ populations while a positive NES indicates enrichment of the specified gene signature in g*Cd8*$^{+}$ cells. T_{FH}-associated gene expression was depleted from *Mll1*-deficient T_{FH} cells (Fig. 5d). Conversely, a T_H1 signature was enriched in *Mll1*-deficient T_{FH} cells (Fig. 5d). Enrichment of a T_H1 gene signature was also observed in *Mll1*-deficient T_H1 cells (Fig. 5d). Genetic signatures associated with T_H2, T_H17 and T_{reg} cells were slightly enriched in *Mll1*-deficient T_{FH} cells (Fig. 5d). In a separate analysis, we observed that wild-type T_H1

cells were enriched for genes upregulated in *Mll1*-deficient cells (Fig. 5e). It was possible that Mll1 controls T_{FH} differentiation by acting in concert with Bcl6 or Blimp-1. We tested the enrichment of Bcl6-bound and Blimp-1 genes in control and *Mll1*-deficient T_H1 and T_{FH} populations but found no strong evidence of Mll1 involvement in the regulation of Bcl6-bound genes (Fig. 5f). Expression of Blimp-1-bound genes was decreased in Mll1-deficient TH1 cells suggesting dysregulation of Blimp-1 activity in the absence of MLL1 (Fig. 5f). Together, these GSEA analyses suggest that in the absence of Mll1, T_{FH} cells gain expression of genes associated with the T_H1 program.

Dysregulated expression of LEF-1 and TCF-1 in *Mll1*-deficient T_{FH}

We searched a curated list of known T_{FH} regulators for genes with dysregulated expression in *Mll1*-deficient T_{FH} cells. *Mll1*-deficient T_{FH} expressed significantly less *Lef1* and *Tcf7*, (Fig. 6a, b). We also observed that *Prdm1*, the gene encoding Blimp-1 had higher expression in *Mll1*-deficient T_{FH} in comparison to control T_{FH} (Fig. 6a). *Id2* and *Il2ra*, two genes associated with suppression of T_{FH} fate (13, 35, 36), were also upregulated in *Mll1*-deficient T_{FH} cells (Fig. 6a). Interestingly, *Lef1* also showed reduced expression in *Mll1*-deficient T_H1 cells (Fig. 6a, b).

GSEA analysis revealed that genes upregulated following ectopic expression of *Lef1* in CD4 T cells are depleted from *Mll1*-deficient T_{FH} cells (Fig. 6c). Conversely, genes suppressed when *Lef1* is overexpressed are over-represented in T_{FH} lacking Mll1 (Fig. 6c). In a separate GSEA analysis, *Mll1*-deficient T_{FH} cells were enriched for genes upregulated in *Lef1*$^{-/-}$ *Tcf7*$^{-/-}$ GC-T_{FH} (Fig. 6d). These findings indicated that LEF-1- and TCF-1-regulated genes were dysregulated, implicating roles for LEF-1 and TCF-1 downstream of Mll1. We measured the expression of LEF-1 and TCF-1 in *Mll1*-deficient T_{FH} cells by flow cytometry. Disruption of *Mll1* reduced expression of both LEF-1 and TCF-1 in early T_{FH} cells (CXCR5$^+$CD25$^-$, Fig. 6e, f, Supplemental Fig. 3a–c) These experiments demonstrate that in the absence of Mll1, LEF-1 and TCF-1 expression is impaired.

We sought to confirm the increased *Prdm1* and *Il2ra* mRNA level in *Mll1*-deficient T_{FH} by analyzing Blimp-1 and CD25 expression by flow cytometry. We first validated the staining of Blimp-1 by showing that CXCR5$^-$CD25$^+$ early T_H1 cells express more Blimp-1 than CXCR5$^+$CD25$^-$ early T_{FH} cells (Supplemental Fig. 3d). We observed sporadic increases in Blimp-1 expression in *Mll1*-deficient CXCR5$^+$Bcl6$^+$ T_{FH} 3 days after LCMV infection (Supplemental Fig. 3e). Similarly, CD25 expression was not reproducibly increased in *Mll1*-deficient T_{FH} (Supplemental Fig. 3f).

TCF-1 partially rescues T_{FH} differentiation of *Mll1*-deficient CD4 T cells

We hypothesized that ectopic expression of Bcl6, TCF-1 or LEF-1 in *Mll1*-deficient CD4 T cells may rescue T_{FH} differentiation, as the expression of all three is decreased in the absence of Mll1. To test this hypothesis, we transduced sh*Cd8*$^+$ and sh*Mll1*$^+$ SMARTA CD4 T cells with RV-*Lef1*, RV-*Tcf7*-p45 (full-length isoform of TCF-1), RV-*Bcl6* or control RV expressing GFP alone. RV$^+$shRNAmir$^+$ SMARTA CD4 T cells were transferred into C57BL/6 recipient mice and T_{FH} differentiation was analyzed 3 days after LCMV-Arm infection. The expression of LEF-1 in sh*Mll1*$^+$*Lef1*-RV$^+$ T_{FH} cells was equivalent to that

of sh*Cd8*$^{+}$GFP^{+} T_{FH} cells (Fig. 7a). As expected, forced expression of LEF-1 resulted in increased T_{FH} differentiation of sh*Cd8*$^{+}$ SMARTA CD4 T cells (Fig. 7b). However, ectopic expression of wild-type levels of LEF-1 in sh*Mll1*$^{+}$ SMARTA CD4 T cells did not rescue T_{FH} differentiation (Fig. 7b). The levels of LEF-1 may not have quantitatively compensated for the reduced levels of TCF-1 (Supplemental Fig. 3g), as *Tcf7* is more highly expressed than *Lef1* at the mRNA level in mouse CD4 T cells (Fig. 6b), supporting a speculation that TCF1 protein is more highly expressed than LEF1.

Expression of *Tcf7*-p45 in *Mll1*-deficient CD4 T cells resulted in TCF-1 expression equivalent to control sh*Cd8*$^{+}$GFP^{+} cells (Fig. 7c). TCF-1 partially rescued the differentiation of early T_{FH} differentiation by *Mll1*-deficient SMARTA CD4 T cells (Fig. 7d), including minimal changes in expression of Bcl6 and LEF-1 (Supplemental Fig. 3h). Overall, the results indicate Mll1 regulates multiple aspects of T_{FH} differentiation, which can only be partially restored by TCF-1 expression.

If Mll1 primarily functions upstream of Bcl6 in T_{FH} differentiation, ectopic expression of Bcl6 may bypass the loss of Mll1 and support T_{FH} differentiation. T_{FH} differentiation of sh*Mll1*$^{+}$ SMARTA CD4 T cells was rescued by ectopic expression of Bcl6 (Fig. 7e) but did not increase LEF-1 and TCF-1 expression in T_{FH} cells (Supplemental Fig. 3i). Overall, these data indicate that Mll1 regulates T_{FH} differentiation by regulating expression of a network of transcription factors that includes, but is most likely not limited to, Bcl6, LEF-1 and TCF-1.

DISCUSSION

Here, we identified Mll1 as a critical regulator of T_{FH} cells. Our work shows that Mll1 is required for optimal T_{FH} cell differentiation and production of IL-21. We demonstrate that absence of Mll1 results in impaired expression of Bcl6, LEF-1 and TCF-1, each of which are important regulators of T_{FH} differentiation. Our findings add Mll1 to the CRs that regulate T_{FH} differentiation (19–24). The results here demonstrate that Mll1 is required for T_{FH} differentiation. Mll1 is also involved in the expression of T_H1 and T_H2 cytokines (33, 34). Thus, Mll1 has roles in multiple CD4 T cell subsets similar to other CRs and transcription factors. The histone methyltransferase EZH2 is required for both T_{FH} and T_{reg} differentiation (21, 22, 37, 38). Similarly, the transcription factors Maf, IRF4 and Batf are all required for both T_H17 and T_{FH} differentiation (9–12, 39, 40).

Accumulation of *Mll1*-deficient CD4 T cells was mildly impaired 3 days after LCMV infection but was more dramatically impaired 3 days later. Loss of Mll1 expression resulted in decreased T_{FH} population at both times analyzed after LCMV infection. It is possible that Mll1 plays a more prominent role in the early stages of T_{FH} differentiation, at a time when the impact of *Mll1*-deficiency on CD4 T cell accumulation is marginal. Mll1 impact on CD4 T cell accumulation may become more prominent at later times as evidenced by decreased BrdU labelling observed 4 days after LCMV infection and the substantial loss in *Mll1*-deficient CD4 T cells 2 days later. Six days after LCMV infection, the decrease in T_{FH} cell frequencies may be secondary to the decreased accumulation of *Mll1*-deficient CD4 T cells. Nevertheless, in a protein immunization system, T_{FH} cells were decreased 8 days after

immunization even when accumulation of CD4 T cells was not impaired in the absence of Mll1.

Our study provides a mechanistic explanation for the defective T_{FH} differentiation in the absence of Mll1. First and foremost, expression of the critical T_{FH} regulator Bcl6 is reduced in *Mll1*-deficient CD4 T cells. A small reduction in Bcl6 expression is sufficient to negatively impact T_{FH} differentiation, as seen in CD4 T cells lacking a single Bcl6 allele (13). The reduced expression of Bcl6 in the absence of Mll1 most likely impairs suppression of alternative cell fates. Partial loss of Bcl6 is probably not the only cause for defective T_{FH} differentiation in the absence of Mll1. LEF-1 and TCF-1 have largely redundant functions to each other in CD4 T cells, and reduced expression of both is likely a key contributing factor to the observed phenotype of *Mll1*-deficient CD4 T cells. Ectopic expression of LEF-1 did not rescue the defective T_{FH} in *Mll1*-deficient CD4 T cells. It is plausible that forced expression of LEF-1 was not elevated enough to compensate for both LEF-1 and TCF-1. TCF-1 is expressed at substantially higher levels than LEF-1 and may explain why ectopic expression of TCF-1 partially compensated for Mll1 deficiency. We suggest that Mll1 controls a network of genes that includes Bcl6, LEF-1 and TCF-1 to promote T_{FH} differentiation. We did not observe any effect of Mll1 on the expression of Bcl6- or Blimp-1-bound genes, suggesting Mll1 does not influence their transcriptional activities. Mll1 may still act on a small subset of such genes and this influence is not detected in our bioinformatics analysis. It is also possible that Mll1 is required for the function of other transcription factors controlling formation of T_{FH} cells.

In addition to driving T_{FH} differentiation, Mll1 promotes production of IL-21. Loss of Mll1 does not impact expression of Maf (data not shown), a transcription factor essential for IL-21 production (11, 12). Deletion of Mll1 could limit H3K4 methylation at the *Il21* locus reducing its transcription leading to impaired production of IL-21. Mll1 is required for normal hematopoiesis (41, 42), but this function does not require the histone methyltransferase domain of Mll1 (43). It is conceivable that the enzymatic activity of Mll1 is not involved in promoting IL-21 production and T_{FH} differentiation.

Chromatin modification is a complex process, and absence of a single CR is often compensated by other enzymes. Reduction in T_{FH} differentiation of *Mll1*-deficient CD4 T cells may be partial due to compensatory mechanisms by other Mll1 family members (Mll2, Mll3 or Mll5), all of which form complexes with Wdr5, Ash2l and RbBp5 (32). Expression of Mll family members and genes coding for components of the Mll1 complex (Wdr5, Ash2l, Dpy30, RbBp5, Menin-1) was normal in the absence of Mll1 (data not shown). The phenotype of *Mll1*-deficient CD4 T cells is similar to the incomplete loss of T_{FH} cells when other CRs are deleted (21–24). Further studies are required to obtain a detailed understanding the role of Mll1 in the control of epigenetic modifications of enhancers and promoters and how this impacts general chromatin accessibility. The roles of members of the Mll1 complex in regulating Mll1 function in the context of T_{FH} differentiation should also be studied.

Disruption of the interaction between Mll1 and the core complex protein Wdr5 with a small molecule drug inhibits the growth of Mll1 leukemic cells (44). Similarly, a small-molecule

inhibitor blocking the interaction between Mll1 and Menin-1 reduces tumor burden in mouse (45). Targeting Mll1 to inhibit T_{FH} differentiation or function could be a promising therapeutic approach for autoimmune disorders characterized by elevated T_{FH} activity. Alternatively, targeting the Mll1 complex to enhance its activity may be used in the design of better vaccines.

Supplementary Material

Refer to Web version on PubMed Central for supplementary material.

ACKNOWLEDGEMENTS

We thank members of the Crotty lab for critical reading of the manuscript, D. Hinz, M. Haynes, S. Sehic, S. Ellis and C. Dillingham of the LJI Flow Cytometry core for cell sorting, K. Fung and J. Greenbaum of the LJI Bioinformatics Core and G. Seumois, H. Simon and A. Wang of the LJI Sequencing core.

The work of S.H. was partially supported by the Achievement Rewards for College Scientists (ARCS) Foundation of San Diego. This work was funded by grants from the USA National Institutes of Health (NIH), including National Institute of Allergy and Infectious Diseases (NIAID) U19 AI109976 and NIAID R01 AI72543, NIH S10 RR027366 (LJI), and internal La Jolla Institute institutional funds to SC.

REFERENCES

1. Crotty S. 2019. T Follicular Helper Cell Biology: A Decade of Discovery and Diseases. Immunity 50: 1132–1148. [PubMed: 31117010]
2. Choi J, Diao H, Faliti CE, Truong J, Rossi M, Bélanger S, Yu B, Goldrath AW, Pipkin ME, and Crotty S. 2020. Bcl-6 is the nexus transcription factor of T follicular helper cells (TFH) via repressor-of-repressor circuits. Nat Immunol 21: 777–789. [PubMed: 32572238]
3. Yu D, Rao S, Tsai LM, Lee SK, He Y, Sutcliffe EL, Srivastava M, Linterman M, Zheng L, Simpson N, Ellyard JI, Parish IA, Ma CS, Li Q-J, Parish CR, Mackay CR, and Vinuesa CG 2009. The transcriptional repressor Bcl-6 directs T follicular helper cell lineage commitment. Immunity 31: 457–468. [PubMed: 19631565]
4. Nurieva RI, Chung Y, Martinez GJ, Yang XO, Tanaka S, Matskevitch TD, Wang Y-H, and Dong C. 2009. Bcl6 mediates the development of T follicular helper cells. Science 325: 1001–1005. [PubMed: 19628815]
5. Johnston RJ, Poholek AC, DiToro D, Yusuf I, Eto D, Barnett B, Dent AL, Craft J, and Crotty S. 2009. Bcl6 and Blimp-1 are reciprocal and antagonistic regulators of T follicular helper cell differentiation. Science 325: 1006–1010. [PubMed: 19608860]
6. Choi YS, Gullicksrud JA, Xing S, Zeng Z, Shan Q, Li F, Love PE, Peng W, Xue H-H, and Crotty S. 2015. LEF-1 and TCF-1 orchestrate T(FH) differentiation by regulating differentiation circuits upstream of the transcriptional repressor Bcl6. Nat Immunol 16: 980–990. [PubMed: 26214741]
7. Xu L, Cao Y, Xie Z, Huang Q, Bai Q, Yang X, He R, Hao Y, Wang H, Zhao T, Fan Z, Qin A, Ye J, Zhou X, Ye L, and Wu Y. 2015. The transcription factor TCF-1 initiates the differentiation of T(FH) cells during acute viral infection. Nat Immunol 16: 991–999. [PubMed: 26214740]
8. Wu T, Shin HM, Moseman EA, Ji Y, Huang B, Harly C, Sen JM, Berg LJ, Gattinoni L, McGavern DB, and Schwartzberg PL 2015. TCF1 Is Required for the T Follicular Helper Cell Response to Viral Infection. Cell Rep 12: 2099–2110. [PubMed: 26365183]
9. Betz BC, Jordan-Williams KL, Wang C, Kang SG, Liao J, Logan MR, Kim CH, and Taparowsky EJ 2010. Batf coordinates multiple aspects of B and T cell function required for normal antibody responses. J Exp Med 207: 933–942. [PubMed: 20421391]
10. Ise W, Kohyama M, Schraml BU, Zhang T, Schwer B, Basu U, Alt FW, Tang J, Oltz EM, Murphy TL, and Murphy KM 2011. The transcription factor BATF controls the global regulators of class-switch recombination in both B cells and T cells. Nat Immunol 12: 536–543. [PubMed: 21572431]

11. Bauquet AT, Jin H, Paterson AM, Mitsdoerffer M, Ho I-C, Sharpe AH, and Kuchroo VK 2009. Costimulatory molecule ICOS plays a critical role in the development of TH-17 and follicular T-helper cells by regulating c-Maf expression and IL-21 production. Nat Immunol 10: 167–175. [PubMed: 19098919]
12. Andris F, Denanglaire S, Anciaux M, Hercor M, Hussein H, and Leo O. 2017. The Transcription Factor c-Maf Promotes the Differentiation of Follicular Helper T Cells. Frontiers in Immunology 8.
13. Shaw LA, Bélanger S, Omilusik KD, Cho S, Scott-Browne JP, Nance JP, Goulding J, Lasorella A, Lu L-F, Crotty S, and Goldrath AW 2016. Id2 reinforces TH1 differentiation and inhibits E2A to repress TFH differentiation. Nat Immunol 17: 834–843. [PubMed: 27213691]
14. Liu X, Chen X, Zhong B, Wang A, Wang X, Chu F, Nurieva RI, Yan X, Chen P, van der Flier LG, Nakatsukasa H, Neelapu SS, Chen W, Clevers H, Tian Q, Qi H, Wei L, and Dong C. 2014. Transcription factor achaete-scute homologue 2 initiates follicular T-helper-cell development. Nature 507: 513–518. [PubMed: 24463518]
15. Lee J-Y, Skon CN, Lee YJ, Oh S, Taylor JJ, Malhotra D, Jenkins MK, Rosenfeld MG, Hogquist KA, and Jameson SC 2015. The transcription factor KLF2 restrains $CD4^+$ T follicular helper cell differentiation. Immunity 42: 252–264. [PubMed: 25692701]
16. Vahedi G, Kanno Y, Furumoto Y, Jiang K, Parker SCJ, Erdos MR, Davis SR, Roychoudhuri R, Restifo NP, Gadina M, Tang Z, Ruan Y, Collins FS, Sartorelli V, and O'Shea JJ 2015. Super-enhancers delineate disease-associated regulatory nodes in T cells. Nature 520: 558–562. [PubMed: 25686607]
17. Weinstein JS, Lezon-Geyda K, Maksimova Y, Craft S, Zhang Y, Su M, Schulz VP, Craft J, and Gallagher PG 2014. Global transcriptome analysis and enhancer landscape of human primary T follicular helper and T effector lymphocytes. Blood 124: 3719–3729. [PubMed: 25331115]
18. Hatzi K, Nance JP, Kroenke MA, Bothwell M, Haddad EK, Melnick A, and Crotty S. 2015. BCL6 orchestrates Tfh cell differentiation via multiple distinct mechanisms. J Exp Med 212: 539–553. [PubMed: 25824819]
19. Nance JP, Bélanger S, Johnston RJ, Hu JK, Takemori T, and Crotty S. 2015. Bcl6 middle domain repressor function is required for T follicular helper cell differentiation and utilizes the corepressor MTA3. Proc Natl Acad Sci U S A 112: 13324–13329.
20. Yang JA, Tubo NJ, Gearhart MD, Bardwell VJ, and Jenkins MK 2015. Cutting edge: Bcl6-interacting corepressor contributes to germinal center T follicular helper cell formation and B cell helper function. J Immunol 194: 5604–5608. [PubMed: 25964495]
21. Li F, Zeng Z, Xing S, Gullicksrud JA, Shan Q, Choi J, Badovinac VP, Crotty S, Peng W, and Xue H-H 2018. Ezh2 programs TFH differentiation by integrating phosphorylation-dependent activation of Bcl6 and polycomb-dependent repression of p19Arf. Nat Commun 9: 5452. [PubMed: 30575739]
22. Chen X, Cao G, Wu J, Wang X, Pan Z, Gao J, Tian Q, Xu L, Li Z, Hao Y, Huang Q, Wang P, Xiao M, Xie L, Tang S, Liu Z, Hu L, Tang J, He R, Wang L, Zhou X, Wu Y, Chen M, Sun B, Zhu B, Huang J, and Ye L. 2020. The histone methyltransferase EZH2 primes the early differentiation of follicular helper T cells during acute viral infection. Cell Mol Immunol 17: 247–260. [PubMed: 30842630]
23. Long X, Zhang L, Zhang Y, Min M, Lin B, Chen J, Ma X, Zhai S, Cai Z, Liu Y, Lu Y, Che N, Tan W, Qin J, and Wang X. 2020. Histone methyltransferase Nsd2 is required for follicular helper T cell differentiation. J Exp Med 217: e20190832.
24. Cook KD, Shpargel KB, Starmer J, Whitfield-Larry F, Conley B, Allard DE, Rager JE, Fry RC, Davenport ML, Magnuson T, Whitmire JK, and Su MA 2015. T Follicular Helper Cell-Dependent Clearance of a Persistent Virus Infection Requires T Cell Expression of the Histone Demethylase UTX. Immunity 43: 703–714. [PubMed: 26431949]
25. Chen R, Bélanger S, Frederick MA, Li B, Johnston RJ, Xiao N, Liu Y-C, Sharma S, Peters B, Rao A, Crotty S, and Pipkin ME 2014. In vivo RNA interference screens identify regulators of antiviral CD4+ and CD8+ T cell differentiation. Immunity 41: 325–338. [PubMed: 25148027]
26. Oxenius A, Zinkernagel RM, and Hengartner H. 1998. Comparison of activation versus induction of unresponsiveness of virus-specific CD4+ and CD8+ T cells upon acute versus persistent viral infection. Immunity 9: 449–457. [PubMed: 9806631]

27. Silva M, Kato Y, Melo MB, Phung I, Freeman BL, Li Z, Roh K, Van Wijnbergen JW, Watkins H, Enemuo CA, Hartwell BL, Chang JYH, Xiao S, Rodrigues KA, Cirelli KM, Li N, Haupt S, Aung A, Cossette B, Abraham W, Kataria S, Bastidas R, Bhiman J, Linde C, Bloom NI, Groschel B, Georgeson E, Phelps N, Thomas A, Bals J, Carnathan DG, Lingwood D, Burton DR, Alter G, Padera TP, Belcher AM, Schief WR, Silvestri G, Ruprecht RM, Crotty S, and Irvine DJ 2021. A particulate saponin/TLR agonist vaccine adjuvant alters lymph flow and modulates adaptive immunity. Sci Immunol 6: eabf1152.

28. Mackay LK, Minnich M, Kragten NAM, Liao Y, Nota B, Seillet C, Zaid A, Man K, Preston S, Freestone D, Braun A, Wynne-Jones E, Behr FM, Stark R, Pellicci DG, Godfrey DI, Belz GT, Pellegrini M, Gebhardt T, Busslinger M, Shi W, Carbone FR, van Lier RAW, Kallies A, and van Gisbergen KPJM 2016. Hobit and Blimp1 instruct a universal transcriptional program of tissue residency in lymphocytes. Science 352: 459–463. [PubMed: 27102484]

29. Jain R, Chen Y, Kanno Y, Joyce-Shaikh B, Vahedi G, Hirahara K, Blumenschein WM, Sukumar S, Haines CJ, Sadekova S, McClanahan TK, McGeachy MJ, O'Shea JJ, and Cua DJ 2016. Interleukin-23-Induced Transcription Factor Blimp-1 Promotes Pathogenicity of T Helper 17 Cells. Immunity 44: 131–142. [PubMed: 26750311]

30. Xiao N, Eto D, Elly C, Peng G, Crotty S, and Liu Y-C 2014. The E3 ubiquitin ligase Itch is required for the differentiation of follicular helper T cells. Nat Immunol 15: 657–666. [PubMed: 24859451]

31. Szabo SJ, Kim ST, Costa GL, Zhang X, Fathman CG, and Glimcher LH 2000. A novel transcription factor, T-bet, directs Th1 lineage commitment. Cell 100: 655–669. [PubMed: 10761931]

32. Dou Y, Milne TA, Ruthenburg AJ, Lee S, Lee JW, Verdine GL, Allis CD, and Roeder RG 2006. Regulation of MLL1 H3K4 methyltransferase activity by its core components. Nat Struct Mol Biol 13: 713–719. [PubMed: 16878130]

33. Yamashita M, Hirahara K, Shinnakasu R, Hosokawa H, Norikane S, Kimura MY, Hasegawa A, and Nakayama T. 2006. Crucial role of MLL for the maintenance of memory T helper type 2 cell responses. Immunity 24: 611–622. [PubMed: 16713978]

34. Schaller M, Ito T, Allen RM, Kroetz D, Kittan N, Ptaschinski C, Cavassani K, Carson WF, Godessart N, Grembecka J, Cierpicki T, Dou Y, and Kunkel SL 2015. Epigenetic regulation of IL-12-dependent T cell proliferation. J Leukoc Biol 98: 601–613. [PubMed: 26059830]

35. Johnston RJ, Choi YS, Diamond JA, Yang JA, and Crotty S. 2012. STAT5 is a potent negative regulator of TFH cell differentiation. J Exp Med 209: 243–250. [PubMed: 22271576]

36. Ballesteros-Tato A, León B, Graf BA, Moquin A, Adams PS, Lund FE, and Randall TD 2012. Interleukin-2 Inhibits Germinal Center Formation by Limiting T Follicular Helper Cell Differentiation. Immunity 36: 847–856. [PubMed: 22464171]

37. DuPage M, Chopra G, Quiros J, Rosenthal WL, Morar MM, Holohan D, Zhang R, Turka L, Marson A, and Bluestone JA 2015. The chromatin-modifying enzyme Ezh2 is critical for the maintenance of regulatory T cell identity after activation. Immunity 42: 227–238. [PubMed: 25680271]

38. Yang X-P, Jiang K, Hirahara K, Vahedi G, Afzali B, Sciume G, Bonelli M, Sun H-W, Jankovic D, Kanno Y, Sartorelli V, O'Shea JJ, and Laurence A. 2015. EZH2 is crucial for both differentiation of regulatory T cells and T effector cell expansion. Sci Rep 5: 10643.

39. Ciofani M, Madar A, Galan C, Sellars M, Mace K, Pauli F, Agarwal A, Huang W, Parkhurst CN, Muratet M, Newberry KM, Meadows S, Greenfield A, Yang Y, Jain P, Kirigin FK, Birchmeier C, Wagner EF, Murphy KM, Myers RM, Bonneau R, and Littman DR 2012. A validated regulatory network for Th17 cell specification. Cell 151: 289–303. [PubMed: 23021777]

40. Krishnamoorthy V, Kannanganat S, Maienschein-Cline M, Cook SL, Chen J, Bahroos N, Sievert E, Corse E, Chong A, and Sciammas R. 2017. The IRF4 Gene Regulatory Module Functions as a Read-Write Integrator to Dynamically Coordinate T Helper Cell Fate. Immunity 47: 481–497.e7.

41. Jude CD, Climer L, Xu D, Artinger E, Fisher JK, and Ernst P. 2007. Unique and independent roles for MLL in adult hematopoietic stem cells and progenitors. Cell Stem Cell 1: 324–337. [PubMed: 18371366]

42. McMahon KA, Hiew SY-L, Hadjur S, Veiga-Fernandes H, Menzel U, Price AJ, Kioussis D, Williams O, and Brady HJM 2007. Mll has a critical role in fetal and adult hematopoietic stem cell self-renewal. Cell Stem Cell 1: 338–345. [PubMed: 18371367]

43. Mishra BP, Zaffuto KM, Artinger EL, Org T, Mikkola HKA, Cheng C, Djabali M, and Ernst P. 2014. The histone methyltransferase activity of MLL1 is dispensable for hematopoiesis and leukemogenesis. Cell Rep 7: 1239–1247. [PubMed: 24813891]

44. Cao F, Townsend EC, Karatas H, Xu J, Li L, Lee S, Liu L, Chen Y, Ouillette P, Zhu J, Hess JL, Atadja P, Lei M, Qin Z, Malek S, Wang S, and Dou Y. 2014. Targeting MLL1 H3 K4 methyltransferase activity in MLL leukemia. Mol Cell 53: 247–261. [PubMed: 24389101]

45. Borkin D, He S, Miao H, Kempinska K, Pollock J, Chase J, Purohit T, Malik B, Zhao T, Wang J, Wen B, Zong H, Jones M, Danet-Desnoyers G, Guzman ML, Talpaz M, Bixby DL, Sun D, Hess JL, Muntean AG, Maillard I, Cierpicki T, and Grembecka J. 2015. Pharmacologic inhibition of the menin-MLL interaction blocks progression of MLL leukemia in vivo. Cancer Cell 27: 589–602. [PubMed: 25817203]

KEY POINTS

- MLL1 is a positive regulator of T_{FH} differentiation
- MLL1 regulates expression of LEF-1, TCF-1 and Bcl6

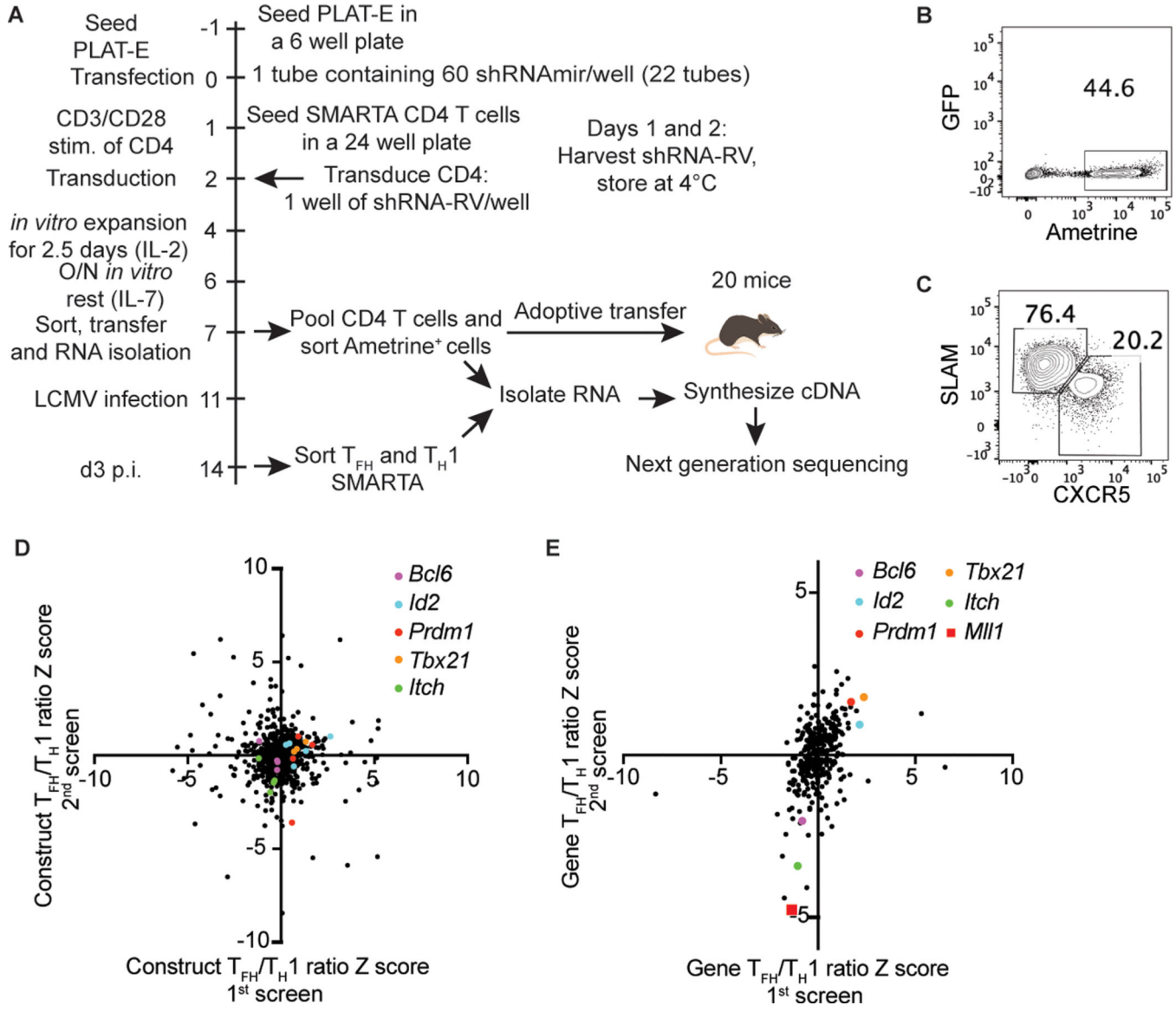

Figure 1: An *in vivo* RNAi screen identifies Mll1 as a novel regulator of T_{FH} differentiation.

(A) Scheme for screening the shRNAmir library targeting CRs. (B) Transduction efficiency of SMARTA CD4 T cells infected with pooled shRNAmir-RV from the CR library. (C) Sorting strategy of shRNAmir$^+$ SMARTA CXCR5$^+$SLAM^{lo} T_{FH} and CXCR5$^-$SLAM$^+$ T_H1 cells 3 days after LCMV infection. (D) Construct T_{FH}/T_H1 ratio Z scores for all shRNAmir in the library in two independent experiments. (E) Gene T_{FH}/T_H1 ratio Z scores for all genes in the library in two independent experiments.

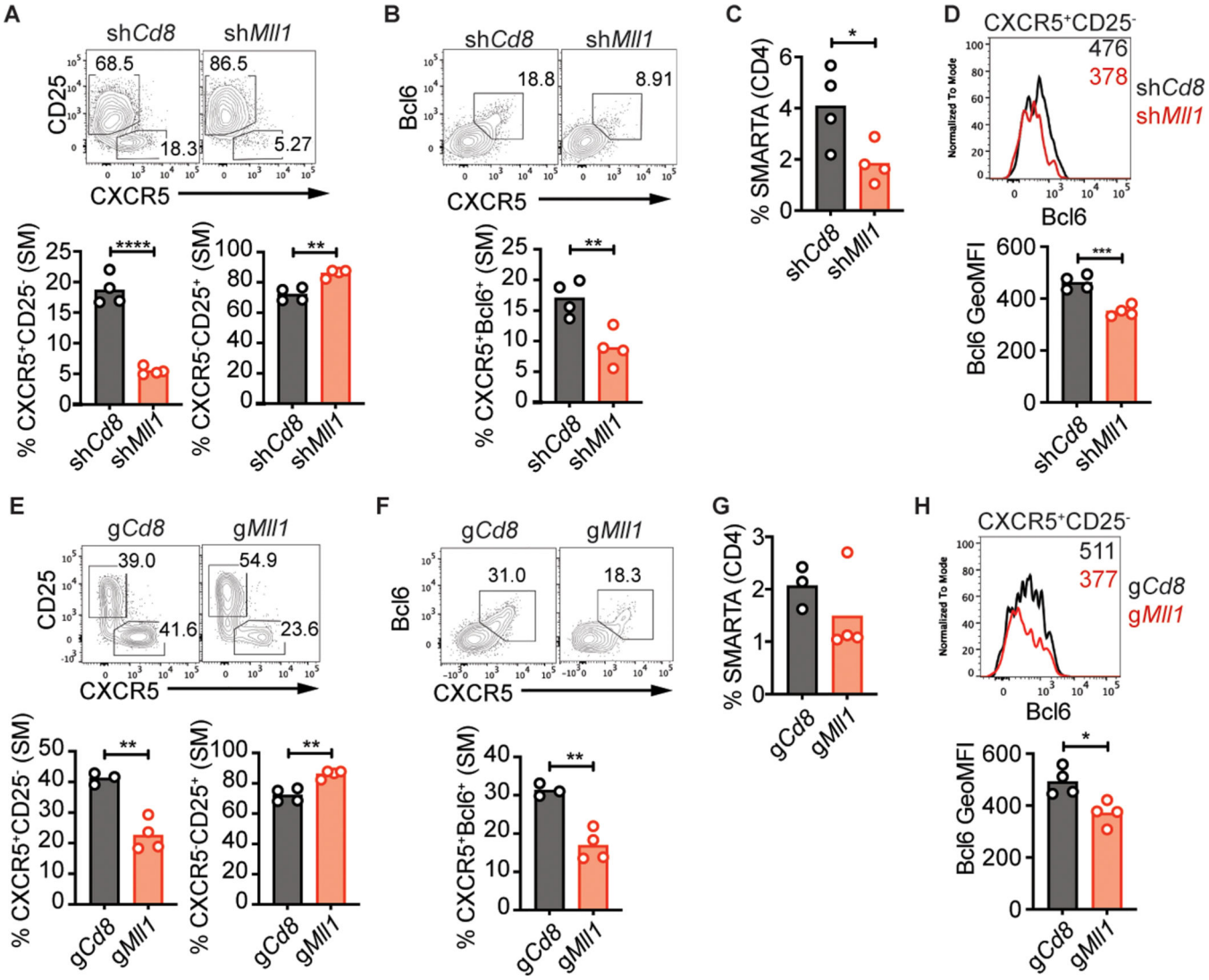

Figure 2: Mll1 is required for proper differentiation of early T_{FH} after LCMV infection.

shRNA$^+$ SMARTA (A-D) or gRNA$^+$ Cas9^{Tg} SMARTA (E-H) CD4 T cells were transferred into C57BL/6 mice and analyzed 3 days after infection with LCMV-Arm. (A) CXCR5$^+$CD25$^-$ T_{FH} and CXCR5$^-$CD25$^+$ T_H1 and (B) CXCR5$^+$Bcl6$^+$ T_{FH} in SMARTA CD4 T cells. (C) Quantitation of SMARTA CD4 T cells. (D) Bcl6 expression in CXCR5$^+$CD25$^-$ SMARTA CD4 T cells. Numbers in the histogram indicate geometric MFI values. (E) CXCR5$^+$CD25$^-$ T_{FH} and CXCR5$^-$CD25$^+$ T_H1 and (F) CXCR5$^+$Bcl6$^+$ T_{FH} in Cas^{Tg} SMARTA CD4 T cells. (G) Quantitation of Cas9^{Tg} SMARTA CD4 T cells. (H) Bcl6 expression in CXCR5$^+$CD25$^-$ Cas9^{Tg} SMARTA CD4 T cells. Data shown are from one experiment representative of 5 (A-D) or 3 (E-H) independent experiments with 3–4 mice per group. *p ≤ 0.05, **p ≤ 0.01, ***p ≤ 0.001, ****p ≤ 0.0001 (unpaired two-tailed Student's t-test).

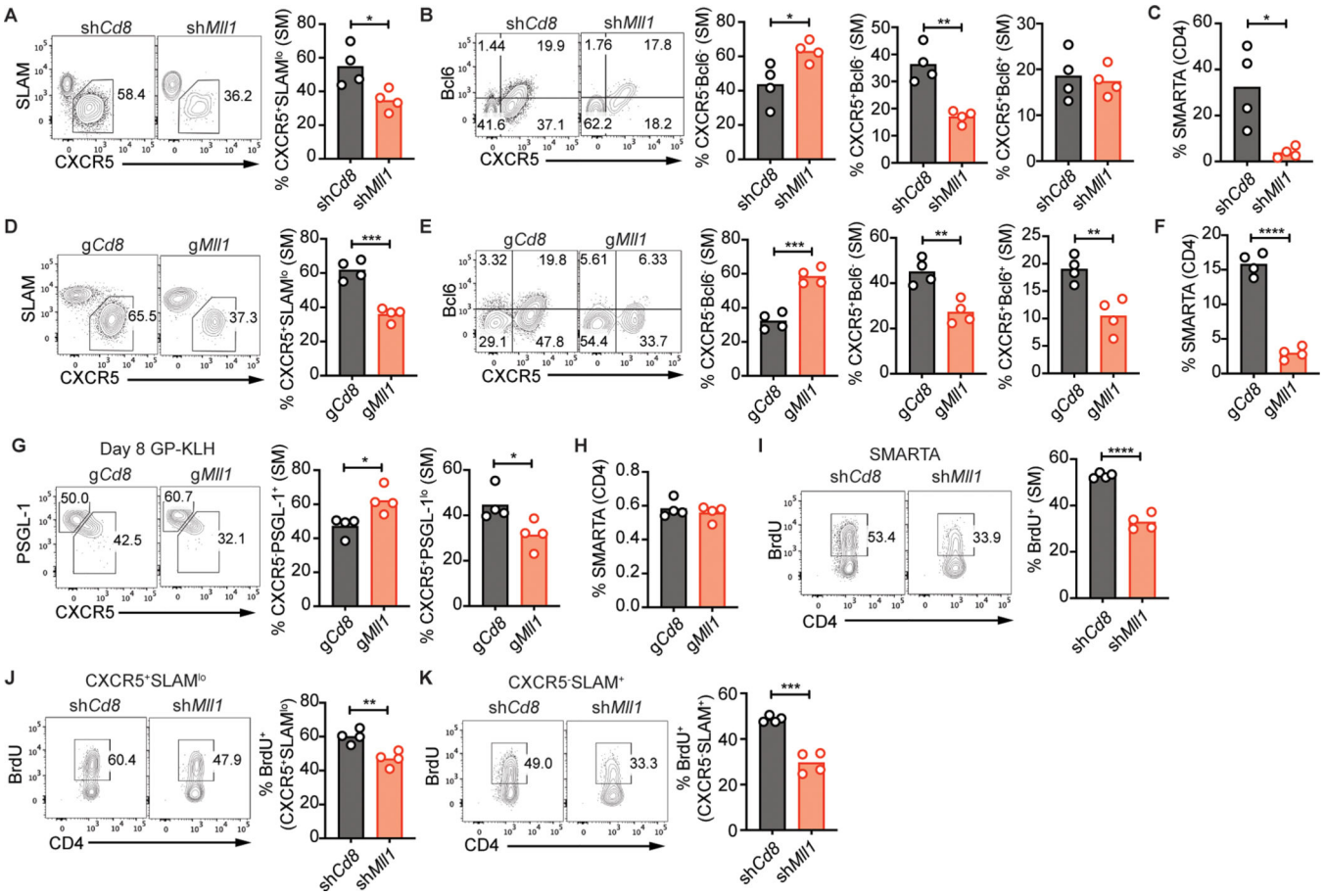

Figure 3: Mll1 is required for proper differentiation of T_{FH}.

shRNA$^+$ SMARTA (A-C) or gRNA$^+$ Cas9^{Tg} SMARTA (D-H) CD4 T cells were transferred into C57BL/6 mice and analyzed 6 days after infection with LCMV-Arm (A-F) or 8 days after immunization with GP-KLH mixed with SMNP (G-H). (A) CXCR5$^+$SLAM^{lo} T_{FH} or (B) CXCR5$^-$Bcl6$^-$ T_H1, CXCR5$^+$Bcl6$^-$ T_{FH} and CXCR5$^+$Bcl6$^+$ GC-T_{FH} in SMARTA CD4 T cells. (C) Quantitation of SMARTA CD4 T cells. (D) CXCR5$^+$SLAM^{lo} T_{FH} or (E) CXCR5$^-$Bcl6$^-$ T_H1, CXCR5$^+$Bcl6$^-$ T_{FH} and CXCR5$^+$Bcl6$^+$ GC-T_{FH} in Cas9^{Tg} SMARTA CD4 T cells. (F) Quantitation of Cas9^{Tg} SMARTA CD4 T cells. (G) CXCR5$^-$PSGL-1$^+$ T_H1 and CXCR5$^+$PSGL-1^{lo} T_{FH} in Cas9^{Tg} SMARTA CD4 T cells. (H) Quantitation of Cas9^{Tg} SMARTA CD4 T cells. (I-K) shRNA$^+$ SMARTA CD4 T cells were transferred into C57BL/6 mice and mice were infected with LCMV-Arm. Mice were injected with BrdU 3 days after infection and analyzed 16 hours later. (I) BrdU$^+$ cells in SMARTA CD4 T cells. (J) CXCR5$^+$SLAM^{lo} T_{FH} SMARTA CD4 T cells and (K) CXCR5$^-$SLAM$^+$ T_H1 SMARTA CD4 T cells. Data shown are from one experiment representative of 5 (A-C), 1 (D-G) or 2 (I-K) independent experiments with 4 mice per group. *p ≤ 0.05, **p ≤ 0.01, ***p ≤ 0.001, ****p ≤ 0.0001 (unpaired two-tailed Student's t-test).

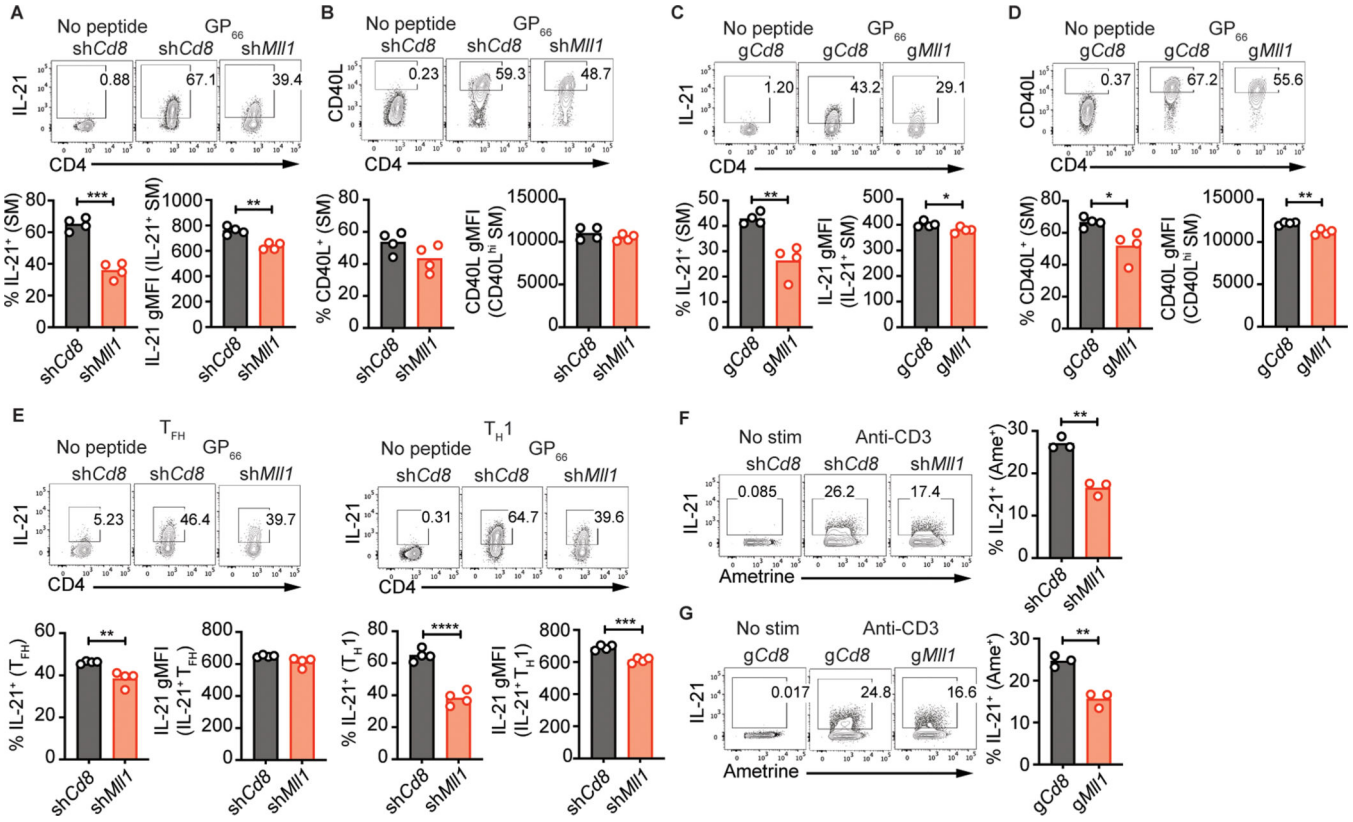

Figure 4: Mll1 is required for production of IL-21.

shRNA$^+$ SMARTA (A-B, E) or gRNA$^+$ Cas9^{Tg} SMARTA (C-D) CD4 T cells were transferred into C57BL/6 mice. 6 days after infection with LCMV-Arm, splenocytes were restimulated with LCMV $gp_{66–77}$ peptide. Expression of IL-21 (A) and CD40L (B) in SMARTA CD4 T cells or T_{FH} and T_H1 SMARTA CD4 T cells (E). Expression of IL-21 (C) and CD40L (D) in Cas9^{Tg} SMARTA CD4 T cells. (F) shRNA$^+$ CD4 T cells were cultured in T_H1 conditions. Expression of IL-21 in shRNA$^+$ CD4 T cells restimulated with anti-CD3. (G) gRNA$^+$ Cas9^{Tg} SMARTA CD4 T cells were cultured in T_H1 conditions. Expression of IL-21 in gRNA$^+$ Cas9^{Tg} SMARTA CD4 T cells restimulated with anti-CD3. Data shown are from one experiment representative of 5 (A-B, E), 3 (C-D) or 2 (F-G) independent experiments with 3–4 mice per group. *p ≤ 0.05, **p ≤ 0.01, ***p ≤ 0.001, ****p ≤ 0.0001 (unpaired two-tailed Student's t-test).

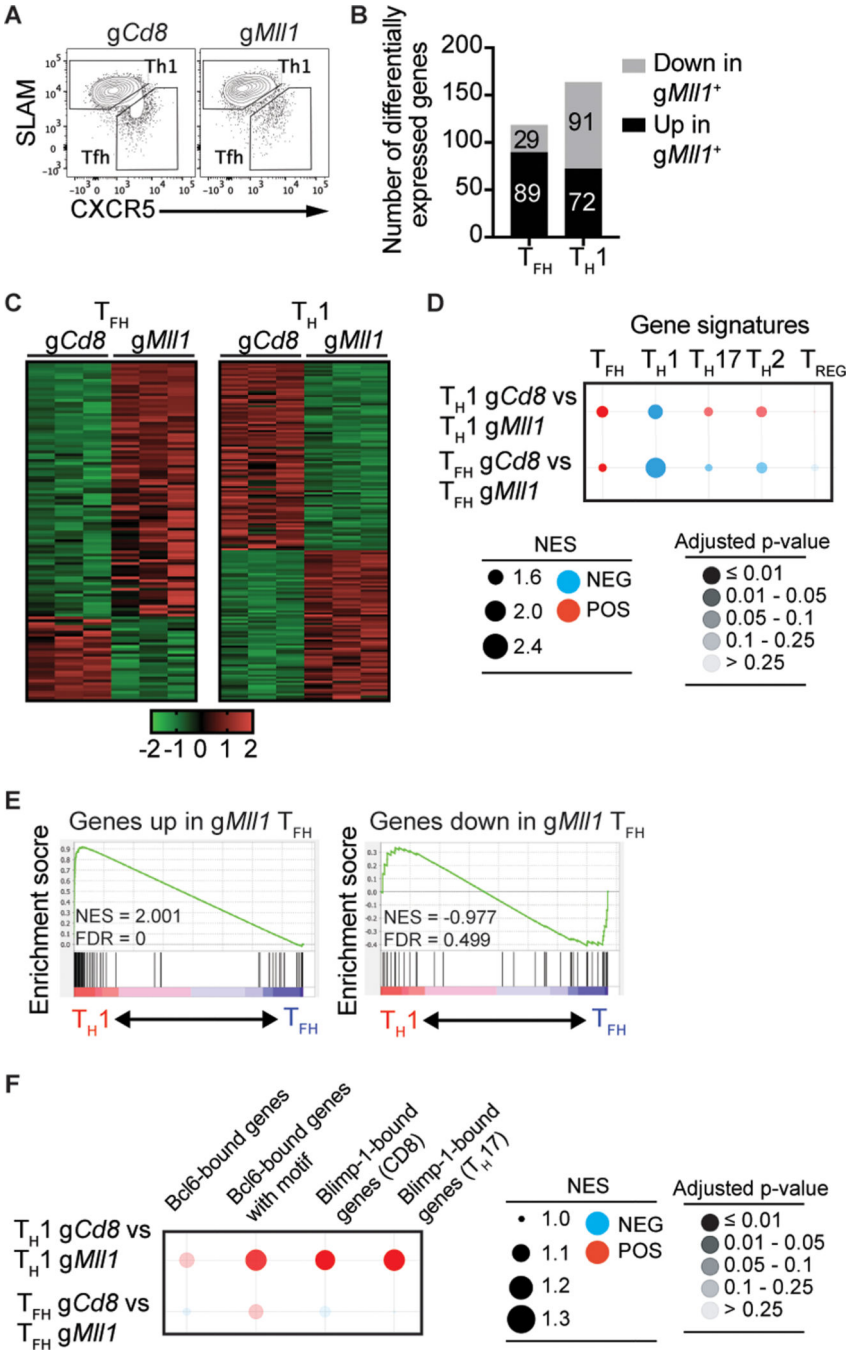

Figure 5: Transcriptomics analysis of *Mll1*-deficient T_{FH}.

(A) gRNA^{+} Cas^{Tg} SMARTA CD4 T cells were transferred into C57BL/6 mice and sorted into CXCR5^{+}CD25^{-} T_{FH} and CXCR5^{-}CD25^{+} T_H1 3 days after infection with LCMV-Arm. (B) Quantitation of differentially expressed genes in g*Cd8*$^{+}$ and g*Mll1*$^{+}$ T_{FH} and T_H1. The numbers of DEGs are indicated in the columns. (C) Heatmaps of differentially expressed genes in g*Cd8* and g*Mll1* T_{FH} and T_H1. (D, F) Bubblegum plots of GSEA analyses of genes differentially expressed between g*Cd8*$^{+}$ and g*Mll1*$^{+}$ T_{FH} or T_H1 against the indicated gene

signatures. (E) GSEA of genes down- or up-regulated in g*Mll1*$^{+}$ T_{FH} compared to genes differentially expressed in g*Cd8*$^{+}$ T_{FH} and T_H1.

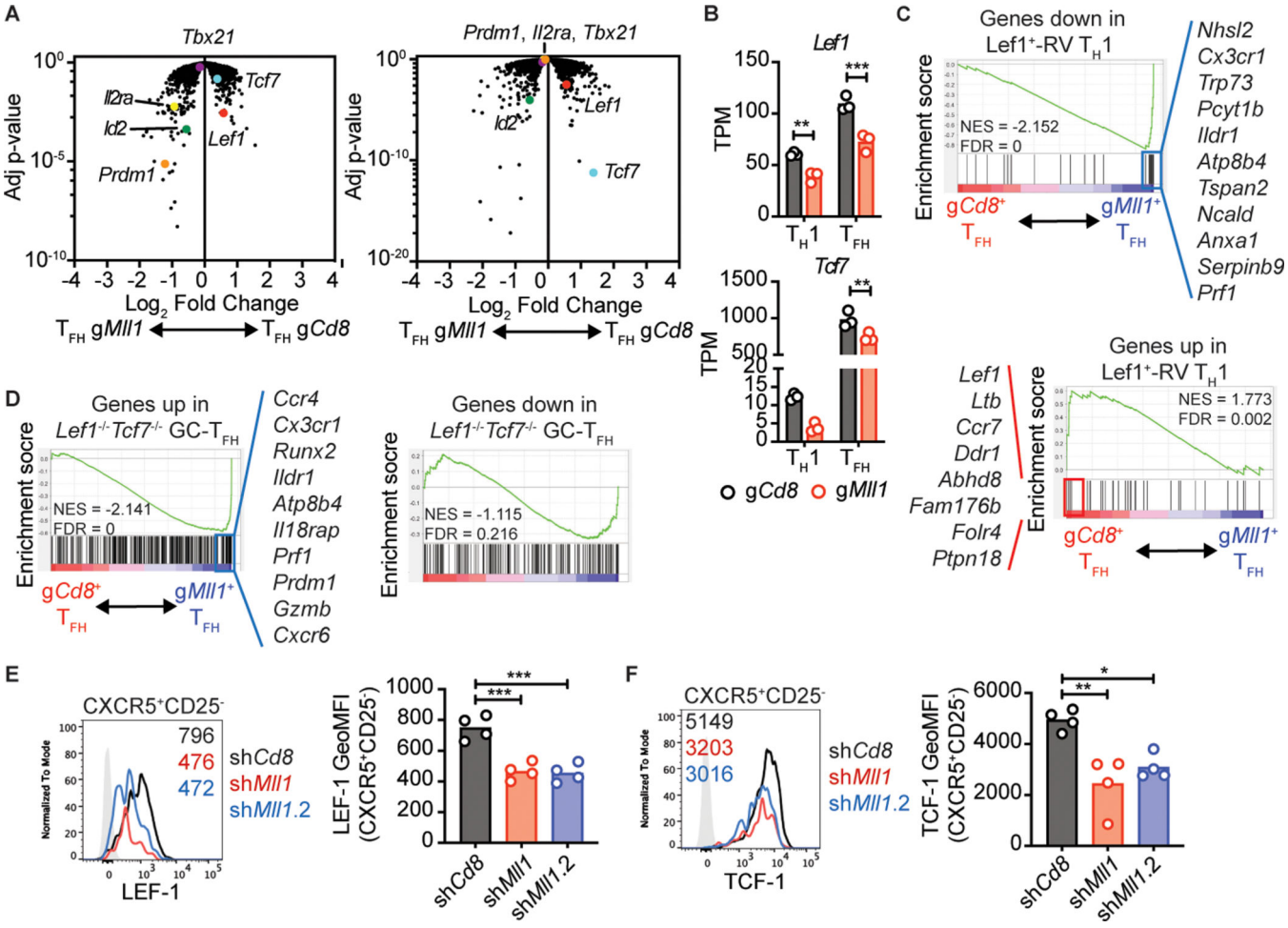

Figure 6: Mll1 regulates expression of LEF-1 and TCF-1 in T_{FH} cells.

(A) Volcano plots of gene expression in g*Cd8*$^+$ and g*Mll1*$^+$ T_{FH} or T_H1 plotted against adjusted p-value. Genes of interest are indicated. (B) TPM values for *Tcf7* and *Lef1* in the indicated populations. (C) GSEA of genes down- or up-regulated in *Lef*-RV$^+$ T_H1 compared to genes differentially expressed in g*Cd8*$^+$ T_{FH} and g*Mll1*$^+$ T_{FH}. (D) GSEA analysis of genes down- or up-regulated in *Lef1*$^{-/-}$ *Tcf7*$^{-/-}$ GC-T_{FH} compared to genes differentially expressed in g*Cd8*$^+$ T_{FH} and g*Mll1*$^+$ T_{FH}. Selected genes that form the core enrichment signatures are listed. (E-F) shRNA$^+$ SMARTA CD4 T cells were transferred into C57BL/6 mice and analyzed 3 days after infection with LCMV-Arm. (E) LEF-1 or (F) TCF-1 expression in CXCR5$^+$CD25$^-$ SMARTA CD4 T cells. Numbers in the histograms indicate geometric MFI values. Data shown are from one experiment representative of 3 (E-F) independent experiments with 4 mice per group. (B) **p ≤ 0.01, ***p ≤ 0.001 (two-way ANOVA with Sidak's multiple comparison test), (E-F) *p ≤ 0.05, **p ≤ 0.01, ***p ≤ 0.001 (one way ANOVA with Tukey's multiple comparisons test).

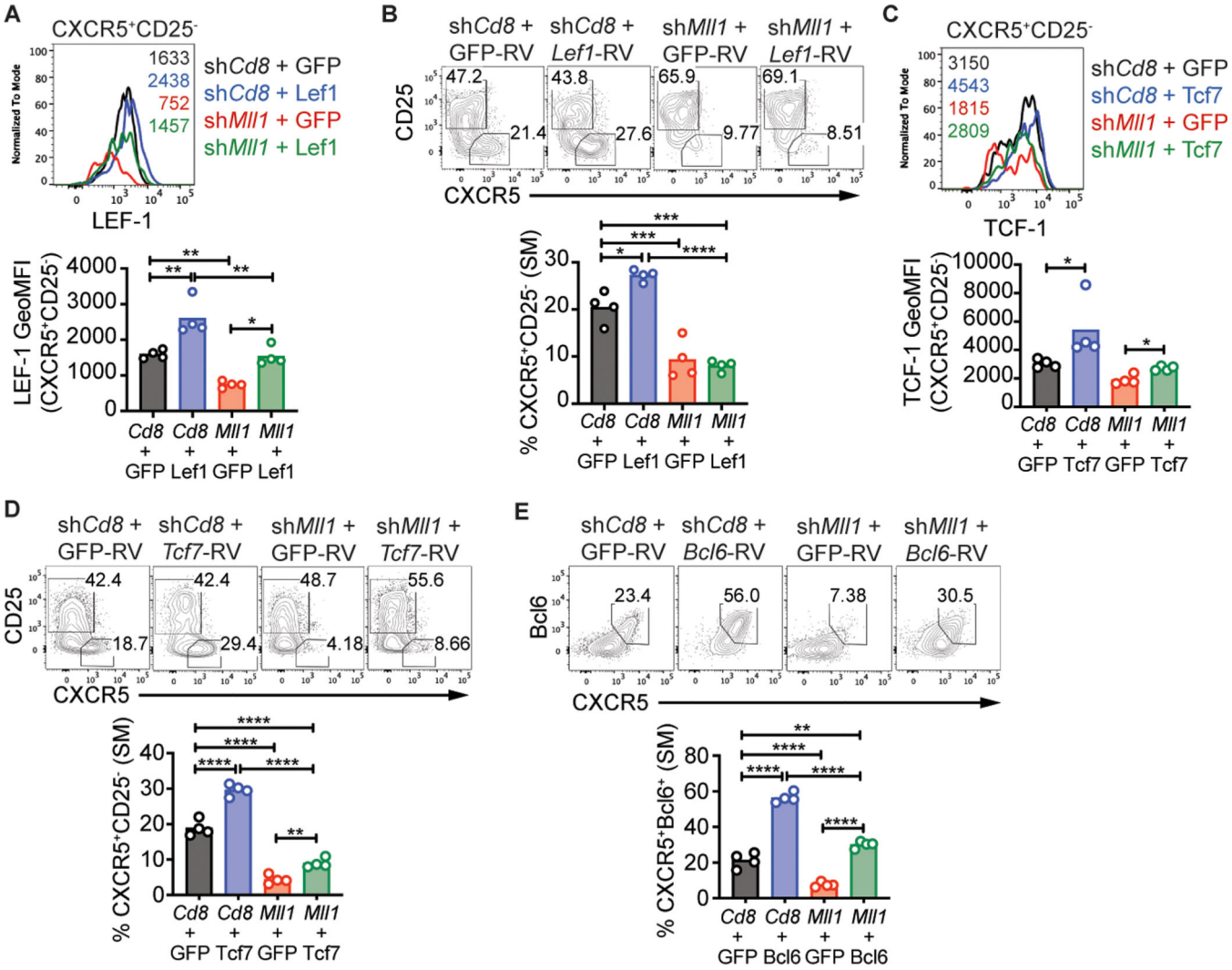

Figure 7: TCF-1 partially rescues T_{FH} differentiation of *Mll1*-deficient CD4 T cells.

SMARTA CD4 T cells transduced with the indicated RV were transferred into C57BL/6 mice and analyzed 3 days after LCMV-Arm infection. (A) LEF-1 or (C) TCF-1 expression in $CXCR5^+CD25^-$ SMARTA CD4 T cells. Numbers in the histogram indicate geometric MFI values. (B,D) $CXCR5^+CD25^-$ T_{FH} or (E) $CXCR5^+Bcl6^+$ T_{FH} in SMARTA CD4 T cells. Data shown are from one experiment representative of 2–3 independent experiments with 4 mice per group. *$p \leq 0.05$, **$p \leq 0.01$, ***$p \leq 0.001$, ****$p \leq 0.001$ (one way ANOVA with Tukey's multiple comparisons test).